Accounting for disturbance history in models: using remote sensing to constrain carbon and nitrogen pool spin-up

Erin J. Hanan [ID],[1,4] Christina Tague [ID],[2] Janet Choate,[2] Mingliang Liu,[1] Crystal Kolden,[3] and Jennifer Adam[1]

[1]*Department of Civil and Environmental Engineering, Washington State University, Pullman, Washington 99164 USA*
[2]*Department of Environmental Science, Policy and Management, University of California Santa Barbara, Santa Barbara, California 93106 USA*
[3]*Department of Geography, University of Idaho, Moscow, Idaho 83844 USA*

Abstract. Disturbances such as wildfire, insect outbreaks, and forest clearing, play an important role in regulating carbon, nitrogen, and hydrologic fluxes in terrestrial watersheds. Evaluating how watersheds respond to disturbance requires understanding mechanisms that interact over multiple spatial and temporal scales. Simulation modeling is a powerful tool for bridging these scales; however, model projections are limited by uncertainties in the initial state of plant carbon and nitrogen stores. Watershed models typically use one of two methods to initialize these stores: spin-up to steady state or remote sensing with allometric relationships. Spin-up involves running a model until vegetation reaches equilibrium based on climate. This approach assumes that vegetation across the watershed has reached maturity and is of uniform age, which fails to account for landscape heterogeneity and non-steady-state conditions. By contrast, remote sensing, can provide data for initializing such conditions. However, methods for assimilating remote sensing into model simulations can also be problematic. They often rely on empirical allometric relationships between a single vegetation variable and modeled carbon and nitrogen stores. Because allometric relationships are species- and region-specific, they do not account for the effects of local resource limitation, which can influence carbon allocation (to leaves, stems, roots, etc.). To address this problem, we developed a new initialization approach using the catchment-scale ecohydrologic model RHESSys. The new approach merges the mechanistic stability of spin-up with the spatial fidelity of remote sensing. It uses remote sensing to define spatially explicit targets for one or several vegetation state variables, such as leaf area index, across a watershed. The model then simulates the growth of carbon and nitrogen stores until the defined targets are met for all locations. We evaluated this approach in a mixed pine-dominated watershed in central Idaho, and a chaparral-dominated watershed in southern California. In the pine-dominated watershed, model estimates of carbon, nitrogen, and water fluxes varied among methods, while the target-driven method increased correspondence between observed and modeled streamflow. In the chaparral watershed, where vegetation was more homogeneously aged, there were no major differences among methods. Thus, in heterogeneous, disturbance-prone watersheds, the target-driven approach shows potential for improving biogeochemical projections.

Key words: carbon cycle modeling; carbon initialization; data model synthesis; disturbance; mechanistic models; post-fire processes; remote sensing; RHESSys; steady-state models; watershed modeling; wildfire.

Introduction

Disturbance is a major force regulating biogeochemical and ecohydrologic dynamics in terrestrial systems. At watershed scales, disturbances interact with range of landscape features to influence carbon (C), nitrogen (N), and water fluxes including vegetation composition and structure, elevation, topography, soil drainage properties, and resource availability (Goodale et al. 2000, Knicker 2007). These features are never homogeneous across watersheds. As a result, watersheds contain a mixture of patches existing at different successional stages. Because ecosystem structure and biogeochemical fluxes vary strongly with successional age, evaluating future C, N, and water balance requires tying together mechanisms that drive biogeochemical and ecohydrologic processes over complex terrain and at multiple scales (Shugart 1984, Pastor and Post 1986, Thomas et al. 2008). Simulation modeling is a powerful tool for bridging these scales; however, model projections are limited by uncertainties in the initial state of plant carbon and nitrogen stores (Hurtt et al. 2004). For models to reliably represent biogeochemical dynamics in disturbance-prone systems, they must be initialized to account for heterogeneous disturbance histories, and non-steady-state conditions.

Watershed models typically use one of two methods to initialize C and N stores prior to simulation. "Spin-up" involves running long simulations to bring C and N pools to steady state given the applied climate forcing (McGuire et al. 1992, Thornton and Rosenbloom 2005, Ajami et al. 2014) and, recently, semi-analytical solutions have been used to reduce the spin-up time required to reach steady state (Xia et al. 2012, Shi et al. 2013). The steady-state approach, however, assumes that vegetation across the entire watershed has reached maturity and is of uniform age. This steady-state assumption may suffice over long (multi-century) time-scales when disturbance regimes are relatively stationary, because C released via combustion and decomposition of dead plant material is eventually replaced through photosynthesis by recovering plants; as such, long-term net C

balance is close to zero (Loehman et al. 2014). However, at temporal scales relevant to managers, steady-state assumptions can severely bias biogeochemical and ecohydrologic projections because ecosystems in the early stages of recovery, for example, will have very different C storage and fluxes than mature ecosystems experiencing similar climate conditions (Kashian et al. 2006, Pietsch and Hasenauer 2006). Furthermore, climate change and changes in disturbance frequency can offset this long-term biogeochemical and hydrologic equilibrium.

Remote sensing has also been used to initialize C and N stores and improve projections of biogeochemical and hydrologic fluxes in non-steady-state systems (Turner et al. 2004, Thomas et al. 2008, Goetz et al. 2009, Antonarakis et al. 2010, Gonzalez et al. 2010). Methods for incorporating remote sensing into model simulations often rely on empirical, allometric or regression relationships between a single vegetation variable (often leaf area index; LAI) and the various C and N stores being modeled (Running and Coughlan 1988, Coughlan and Dungan 1997, Hurtt et al. 2004, Tague and Band 2004). However, these relationships can sometimes be problematic, because they are species- and site-specific. When applied at large scales, they do not account for local resource availability and site conditions (including local climate, soil water-holding capacity, groundwater accesses, etc.), which can influence C allocation to leaves, stems, and roots (Motallebi and Kangur 2016). For example, two patches may have identical LAI; in one patch, the LAI may be limited by temperature, in the other by water availability, even within the same watershed. The vegetation growing in the dry location would likely allocate more C belowground to maximize access to water. If researchers derive allometric relationships (as a function of LAI) based on region-wide data, root C may be underestimated in the water-limited site, resulting in C and N distributions that are unrealistic. In the worst-case scenario, starting a simulation with this initial root C may be unstable, causing vegetation biomass to rapidly decline because roots cannot access enough water to support photosynthesis estimates that are large enough to cover the respiration costs required by the initialized aboveground C stores. In addition, because allometric relationships derive C stores from a single measured variable (e.g., LAI), they cannot draw on multiple data products, which may be invaluable for improving the way we initialize vegetation structure in disturbance-prone watersheds.

To address the potential limitations associated with commonly used spin-up strategies, and to provide a method for integrating multiple state-of-the-art data products, we developed a novel approach for initializing vegetation C and N stores in biogeochemical models using the spatially distributed, ecohydrologic model RHESSys (Tague and Band 2004). In this approach, one or more vegetation variables derived from a spatial data layer, such as LAI from Landsat or MODIS, stem wood from LiDAR, or stand age maps, can be used to define spatially explicit targets for individual landscape units (i.e., patches) across a watershed. Then, a spin-up implementation of the model is used to simulate plant growth and track C and N stores in each patch until they reach these targets. Once all patches have reached their targets, the model outputs state variables that can be used to initialize subsequent simulations. This approach allows C

and N pools to develop mechanistically over time, accounting for the effects of local resource and climate variability. Additionally, unlike traditional spin-up, which assumes steady-state conditions, the new approach uses remote sensing to spatially constrain pool sizes. Thus, the new approach supports heterogeneous stand ages that are characteristic of disturbance-prone systems.

Here, we present our new target-driven initialization approach. Then, as a first evaluation, we compare model estimates of C, N, and water fluxes using the new approach to those using the two previously established methods (spin-up to steady state and remote sensing coupled with allometric relationships). We also compare model estimates of streamflow following initialization with observation-based estimates. Specifically, we address the following questions: (1) How do projected LAI, rooting depth, evapotranspiration, streamflow, and N export vary among simulations using the three different approaches for initializing C and N pools? (2) In years following initialization, does the new target-driven approach provide similar or improved correspondence between modeled and observed streamflow relative to previously established approaches? We then discuss potential further applications of our approach that would integrate data from a wide range of emerging remote sensing products.

METHODS

Study sites

We implemented our spin-up approaches and compared estimates of C, N, and hydrologic dynamics in two fire-prone watersheds in the western United States. The first watershed, Johnson Creek, is a 565-km^2 subcatchment of the South Fork Salmon River, which is part of the larger Columbia River Basin. Johnson Creek is located in Valley County, Idaho along the southern boundary of Payette National Forest and the northern boundary of Boise National Forest (44°58′ N, 115°30′ E; Fig. 1a). The region is characterized by cold winters with heavy snowfall, which constitutes ~65% of annual precipitation. Summers are hot and dry with most warm-season precipitation falling during high-intensity thunderstorms (Megahan et al. 1992). Mean annual precipitation in the region is ~680 mm, however rainfall varies substantially between wetter montane forests and semiarid interior valleys. Johnson Creek is located within the Idaho batholith, where steep slopes and granitic bedrock produce shallow coarse-textured soils (Hyndman 1983). Elevations range from 1,429 to 2,779 m. Vegetation is mixed pine species, dominated by ponderosa pine (*Pinus ponderosa*) and Douglas-fir (*Pseudotsuga menziesii*) at lower elevations, and lodgepole pine (*Pinus contorta* var. *latifolia*), grand fir (*Abies grandis*), Engelmann spruce (*Picea engelmannii*), and subalpine fir (*Abies lasiocarpa*) at higher elevations (Arkle and Pilliod 2010). Riparian, shrub, and herbaceous species are also present (Homer et al. 2015). Most fires in the region are either mixed severity or stand replacing (surface fires are relatively rare); stand-replacing fires occur on average every 200 yr (Rollins 2009). Eleven fires burned portions of the watershed between 1989 and 2015; the two largest being the Thunderbolt fire in 1994 and Cascade Complex in 2007 (Eidenshink et al. 2007).

The second site, Rattlesnake Canyon, is a chaparral-dominated, 6-km^2 subcatchment of the Mission Canyon watershed, located in the Santa Ynez Mountains in southern California (34°28′ N, 119°40′ W; Fig. 1b). The region has a Mediterranean climate with cool wet winters and hot dry summers. Mean annual precipitation ranges from 500 mm/yr at lower elevations to 850 mm/yr at higher elevations, 80% of which typically falls between December and March (Beighley et al. 2005). Elevations in Rattlesnake Canyon range from 270 to 1,262 m, and slopes are steep (>20%). Soils in the region are classified as Typic Dystroxerepts from the Maymen series (NRCS 2015). These sandy loam soils are weathered from shale, schist, greenstone, sandstone, and conglomerate. They are rocky, nutrient poor, shallow, well drained, and highly erosive. Vegetation in Rattlesnake Canyon includes evergreen shrubs, dominated by big pod ceanothus (*Ceanothus megacarpus*), chamise (*Adenostoma fasciculatum*), and manzanita (*Arctostaphylos* spp.). These species are well adapted to crown fires, which consume most aboveground vegetation. Fire return intervals typically range from 40 to 60 yr (Moritz 2003). Most of Rattlesnake Canyon burned in the 2009 Jesusita Fire, and a small portion burned in the 2008 Tea Fire. Prior to these fires, the watershed last burned in the 1964 Coyote Fire.

RHESSys model

Model development and simulations for this study were conducted using RHESSys. RHESSys is a spatially distributed, mechanistic model that couples ecohydrologic and
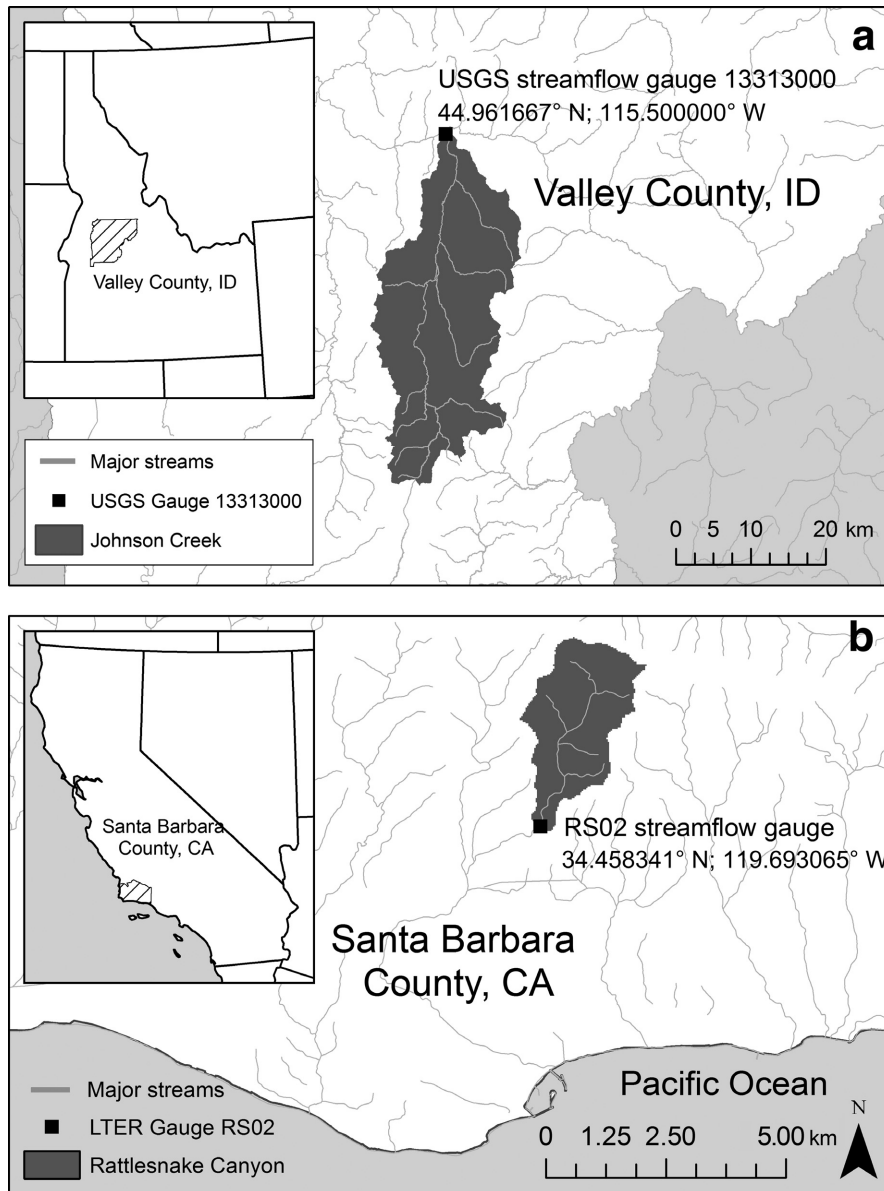

Fig. 1. Study sites include (a) the Johnson Creek watershed, which is a subcatchment of the Southfork Salmon River within the Columbia River Basin in Valley County, Idaho (ID) and (b) the Rattlesnake Canyon watershed, which is nested within the upper reach of Mission Canyon in the Santa Ynez Mountains in Santa Barbara County, California, USA.

biogeochemical processes to simulate water, C, and N fluxes such as streamflow, evapotranspiration, photosynthesis, respiration, NPP, and N export at watershed scales. RHESSys has been rigorously tested and run in mountainous regions, including watersheds in the Pacific Northwest and California chaparral (Tague et al. 2004, 2009, Shields and Tague 2012, Abdelnour et al. 2013, Garcia et al. 2013, 2016, Hanan et al. 2017).

RHESSys partitions a watershed into a hierarchical set of spatial units representing the scale at which different hydrologic and biogeochemical processes are modeled (Tague and Band 2004). Vertical soil moisture and soil biogeochemistry are modeled at the finest spatial scale (the patch). Meteorological forcings (time-varying inputs) are also organized at the patch level, and are modified by elevation, slope, and aspect. Hillslopes aggregate explicit routing between patches to produce streamflow, and are defined as areas that drain into one side of a single stream reach. For our application, meteorological inputs include daily maximum and minimum temperature and precipitation. Vapor pressure deficit (VPD) and incoming radiation are calculated by RHESSys using standard air-temperature–VPD relationships (Jones 2013) and the MTN-CLIM approach (Running et al. 1987), respectively. The largest spatial unit is the basin, which is a closed drainage area encompassing a single stream network.

RHESSys uses geospatial data including a digital elevation model (DEM), as well as soil and landcover maps, to delineate biophysical characteristics across a watershed. It extrapolates spatial variation in climate inputs across the terrain using lapse rates (Tague and Band 2004). RHESSys then models vertical and lateral hydrologic fluxes, including rainfall interception, snow accumulation, snowmelt, infiltration, evapotranspiration (using a Penman-Monteith approach (Monteith 1965), and subsurface drainage. Vertical and lateral drainage respond to topography and soil hydraulic conductivity, which decreases exponentially with depth.

Biogeochemical processes in RHESSys include C cycling and corollary N dynamics. Photosynthesis is estimated using the Farquhar model (Farquhar and Von Caemmerer 1982) and, in this study, a portion of net photosynthate is allocated to leaves, stems, and roots each day according to the Dickinson partitioning strategy, which accounts for changes in allocation that occur as a plant matures (Dickinson et al. 1998). The remaining portion of net photosynthate is stored and expressed during an annual leaf-out period. RHESSys estimates of LAI are based on simulated leaf C and a species-specific leaf area parameter. Transpiration and photosynthesis are both influenced by stomatal conductance, which varies in response to soil water availability, VPD, atmospheric CO_2 concentration, radiation, and temperature (Jarvis 1976). These relationships couple plant productivity with climate and hydrology. Decomposition submodels are modified from BIOME-BGC and CENTURY-NGAS. These include litter and soil C and N dynamics, such as respiration, mineralization, nitrification, and denitrification (Parton 1996, Nemani et al. 2005). Tague and Band (2004) provide a detailed description of the hydrologic, ecophysiological, and biogeochemical algorithms used to estimate the above processes.

Modeling framework for initializing C and N pools

In the previous version of RHESSys, users could choose between the two commonly used methods for initializing vegetation C and N stores: (1) they could spin pools up from zero until they reached steady state (Tague and Band 2004) or (2) users could initialize carbon pools with allometric tables to assign C and N stores as a function of remotely sensed LAI (Fig. 2).

In the new target-driven spin-up approach, we use a vegetation spatial data layer to define one or more targets for each patch. Targets are defined broadly to allow for the use of a wide range of possible C and or N observations. Any RHESSys C or N store (e.g., leaf C, stem N, etc.) or combination of stores (e.g., above ground biomass) can be used. The user can also specify multiple targets (e.g., leaf C and stem C). Possible RHESSys state variables are listed in Table 1. A spin-up implementation of the model is then used to grow all stores from near zero values (a small initial value (e.g., 0.004 kg C/m^2) for leaf and root C are required to initiate growth). The spin-up implementation of the model then simulates growth for each patch using site-specific climate inputs and vegetation/soil parameters. Plant C and N stores are tracked for each patch until they reach their target(s). When an individual patch reaches its target(s), values for all of the C and N pools are stored in a separate location while all other patches in the basin continue to grow and accumulate C and N

$$CN_{stored} = CN \text{ when } CN_{tracked} \geq target_x \\ - \tau(target_x) \& T \leq T_{max}. \tag{1}$$

In this equation, CN_{stored} represents the values for each of the C and N pools that are stored when a given patch reaches its target(s). $CN_{tracked}$ represents the state variable(s) being tracked; τ represents tolerance, which is a user-defined parameter that sets the allowable error between the parameter(s) being tracked during spin-up and the target value(s). The default value for τ is 0.05. Thus, the target is reached when model estimate of the target variable (e.g., LAI) is within 5% of the user-specified target(s) for a given patch.
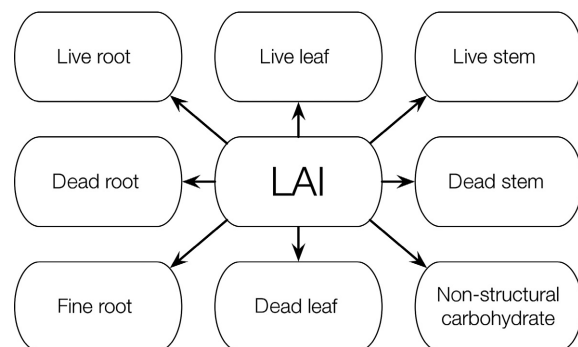

Fig. 2. Illustration of how remote sensing such as leaf area index can be used to allocate C and N to the various carbon and nitrogen stores in models. Leaf area index (LAI) is generally measured using remote sensing and C and N stores subsequently are calculated using allometric relationships.

Table 1. List of RHESSys state variables that can be used for assigning spin-up targets, and potential sources for acquiring these measurements.

Store and variable	Source
C	
Leaf	hyperspectral remote sensing (e.g., AVIRIS)
Stem	active remote sensing (e.g., lidar)
Root	active remote sensing (e.g., ground-penetrating radar), field measurements
N	
Leaf	hyperspectral remote sensing
Stem	combined hyperspectral and active remote sensing
Root	field measurements
Combined	
Aboveground biomass	multispectral remote sensing (e.g., MODIS, Landsat), hyperspectral remote sensing, active remote sensing
Leaf Area Index	multispectral remote sensing, hyperspectral remote sensing, active remote sensing
Canopy height	active remote sensing
Stand age	field surveys

Note: Users can define one or more targets from this list.

The parameter τ can be changed to reflect greater or lesser confidence in the accuracy or precision of the user-specified target. Note that, because RHESSys estimates are increasing toward the target, we use τ to define a lower bound, however, it is possible to go beyond the target if the value being tracked exceeds the target in a given time step. Once the target is exceeded, the current carbon and nitrogen values are stored. T represents the length of time the model has been spinning up and T_{max} is an additional user-defined parameter that sets limits on the length of spin-up time. Where data are missing, vegetation is allowed to spin up to steady state (or as long as is defined by the parameter T_{max}).

Once all patches have reached their targets, the model outputs the state variables, including the appropriate C and N stores, for all patches. These state variables can then be used to initialize subsequent simulations. This approach allows patches to differ from one another in terms of the number of years required for spin-up, thus supporting non-homogeneous stand ages, while still allowing C and N stores to develop mechanistically over time.

Input data

We derived landscape topographic characteristics including elevation, slope, and aspect for each watershed from a digital elevation model downloaded from the U.S. Geologic Survey National Elevation Data set at 10-m resolution.[5] Basin boundaries, hillslopes, and patches were then delineated in GRASS GIS (GRASS Development Team, http://grass.osgeo.org) using the watershed analysis program, r.watershed. For Johnson Creek, we aggregated topographic data to generate patches with an average size of 30 m^2 and 270 m^2 in riparian and upslope areas, respectively. This

[5] https://nationalmap.gov/elevation.html

approach allowed us to maximize computational efficiency in a relatively large watershed, while still maintaining fine resolution in key regions (Tague et al. 2004). Johnson Creek contained 189,872 patches, organized into 275 hillslopes of varying sizes (mean = 0.49 km^2). In Rattlesnake Canyon, all patches were aggregated to 30 m^2, resulting in 6,095 patches that were organized into 34 hillslopes (mean size = 0.17 km^2). Vegetation land cover from the National Land Cover Database (NLCD; Homer et al. 2015) was aggregated to six types in Johnson Creek: conifer, grass/herbaceous, shrub, deciduous, open water, and rock. Vegetation was aggregated to one type (shrub) in Rattlesnake Canyon. Soil and vegetation parameters for these land cover types were assigned based on literature (Law et al. 2003, Ackerly 2004, Vourlitis et al. 2007, Berner and Law 2016, Hanan et al. 2016a, b) and existing spatial data layers (White et al. 2000, Tague et al. 2009).

For Johnson Creek, we acquired daily, high-resolution (1/24th degree or ~4 km) gridded meteorological data, namely, precipitation and maximum and minimum temperatures for water years 1980–2014 (Abatzoglou 2013). This data set combines the spatial attributes of gridded climate data from PRISM (Daly et al. 1994) with temporal attributes of regional-scale reanalysis and daily gauge-based precipitation from NLDAS-2 (Mitchell et al. 2004, Abatzoglou and Brown 2012, Abatzoglou 2013). For Rattlesnake Canyon, climate data for water years 2001–2013 is composed of daily gauge-based precipitation data taken from the nearby Stanwood Fire Station and daily temperature data taken from the National Climate Data Center (NCDC) Santa Barbara monitoring site near the harbor (Fig. 1b). We generated climate data for long simulations by repeating the available 34-yr meteorological record in Johnson Creek, and the 13-yr record in Rattlesnake Canyon. We also collected streamflow data from USGS gage no. 13313000 for Johnson Creek and Santa Barbara Coastal Long Term Ecological Research Network Gauge no. RS02 for Rattlesnake Canyon (Fig. 2a, b).

We used a Monte Carlo approach to calibrate four shallow subsurface soil parameters: saturated hydraulic conductivity (K_{sat}), decay of K_{sat} with depth (m), air-entry pressure (φ_{ae}), and pore size index (b), as well as two parameters used to define bypass flow to deeper groundwater stores (gw1) and groundwater drainage rates to the stream (gw2). In Johnson Creek, we selected the best parameter set by comparing observed and modeled streamflow using the Nash-Sutcliffe efficiency metric (NSE; Nash and Sutcliffe 1970), NSE of log transformed flows (to evaluate low flow periods), R^2 for the correlation between daily observed and modeled flow, and percent error in annual flow estimates. In Rattlesnake Canyon, prior hydrologic modeling studies found that peak flow estimates were highly sensitivity to precipitation input and model sensitivity to soil drainage and storage parameters was greatest during streamflow recession (Shields and Tague 2012). Given the potentially large uncertainty and error in precipitation input data in this semi-arid region, we found that calibrating on recession periods provided a more robust estimation of drainage parameters. In Rattlesnake Canyon, we extracted recession periods, and then selected the best parameter set by comparing observed and modeled streamflow using NSE of log-transformed flows and percent error in annual flow estimates.

Remote sensing

For this study, we based targets on LAI. We calculated LAI for Johnson Creek and Rattlesnake Canyon using the best available remote sensing scenes for each region. To produce peak-growing season LAI input layers for initializing Johnson Creek, we used Landsat-7 Enhanced Thematic MapperPlus (ETM+) surface reflectance data generated at 30-m resolution, acquired on 8 August 2001 for WRS2 path/row 41/29. We calculated a Normalized Difference Vegetation Index (NDVI) for the 2001 reflectance data using

$$NDVI = \frac{(\rho_{NIR} - \rho_R)}{(\rho_{NIR} + \rho_R)} \qquad (2)$$

where ρ_{NIR} represents reflectance in the near infrared portion of the electromagnetic spectrum and ρ_R represents reflectance in the red.

In Rattlesnake Canyon, we acquired hyperspectral remote sensing imagery collected at 12 m resolution by the Airborne Visible/Infrared Imaging Spectrometer (AVIRIS; Green et al. 1998) on 6 August 2004. The AVIRIS scene was atmospherically corrected, converted to reflectance and geo-rectified (D. A. Roberts, *unpublished data*). We calculated NDVI using Eq. 1. For both Landsat 7 ETM+ and AVIRIS, the ρ_{NIR} band is centered at 830 nm, and ρ_R band is centered at 660 nm.

To transform NDVI to LAI, we used a generalized NDVI-LAI model developed by Baret et al. (1989: Eq. 3). This model has been used to convert NDVI into LAI values in chaparral, oak woodland, and other ecosystems (Gamon et al. 1995, Garson and Lacaze 2003, McMichael et al. 2004)

$$LAI = -\frac{1}{k} \times \ln\left(\frac{NDVI_\infty - NDVI}{NDVI_\infty - NDVI_{back}}\right). \qquad (3)$$

In Eq. 3, k is a parameter corresponding to the extinction of solar radiation through a canopy, $NDVI_\infty$ is the maximum NDVI observed in each region, and $NDVI_{back}$ is the background NDVI (in the absence of vegetation) for each region. We parameterized this model for each vegetation type in each image (Table 2). The parameter (k) was estimated from Smith et al. (1991) for mixed pine vegetation and from White et al. (2000) for all other vegetation types. To avoid bias introduced by outliers, $NDVI_{back}$ was set equal to the average NDVI of the 20 brightest soil/rock pixels in each image.

C and N initialization and simulations

Prior to testing the three approaches, we initialized organic soil C and N stores with small values and then ran a preliminary spin-up to allow the three fastest-cycling soil C pools to approach steady state (~500 yr). We generated climate data for these simulations by repeating the available meteorological record for each watershed. After stabilizing soil biogeochemical processes, we removed vegetation C and N stores and proceeded with three methods for initializing plant C and N stores: spin-up to steady state, remote sensing

TABLE 2. Normalized difference vegetation index-leaf area index (NDVI-LAI) model parameters for vegetation types in Johnson Creek and Rattlesnake Canyon. $NDVI_\infty$ is the maximum NDVI observed in each region, and $NDVI_{back}$ is the background NDVI (in the absence of vegetation) for each region.

Vegetation	k	2001 $NDVI_\infty$	2001 $NDVI_{back}$
Johnson Creek†			
Pine	0.40	0.98	0.07
Grass	0.59	0.90	0.07
Shrub	0.55	0.90	0.07
Deciduous	0.54	0.88	0.07
Rattlesnake Canyon			
Shrub	0.55	0.92	0.11

Note: $NDVI_\infty$ is the maximum NDVI observed in each region and $NDVI_{back}$ is the background NDVI (in the absence of vegetation) for each region.
†$NDVI_\infty$ and $NDVI_{back}$ from 2001.
‡$NDVI_\infty$ and $NDVI_{back}$ from 2004.

with allometric relationships, and the new target-driven spin-up approach.

Spin-up to steady state.—For the traditional steady-state spin-up approach, we ran 200-yr and 50-yr spin-up simulations in Johnson Creek and Rattlesnake Canyon, respectively. These timespans allowed above- and belowground vegetation C and N stores to reach steady state and corresponded with the fire return interval (for stand-replacing fires) in each watershed.

Allometric relationships.—For the allometric approach, we used the LAI maps generated for each watershed and allocated C and N to leaves, stems, and roots using allometric ratios for each vegetation type, summarized in Table 3.

Target-driven spin-up.—For the target-driven spin-up, we used the same LAI maps to define targets for each patch, and then ran RHESSys in spin-up mode, tracking C and N stores for each patch separately until they reached their target. For the target-driven spin-up runs, we set T_{max} to 200 yr for Johnson Creek and 100 yr for Rattlesnake Canyon.

We ran three 50-yr simulations for both watersheds, each using one of the three initialization methods. To examine differences among the three methods, we compared decadal scale LAI, ET, NPP, streamflow, and N export. To evaluate model performance in Johnson Creek, we compared modeled and observed streamflow during a portion of the 50-yr simulation in each watershed where we had both climate and streamflow data, and excluded years that experienced (or followed) stand-replacing fires. In Johnson Creek, this included water years 2002–2006 (i.e., simulation years 0–5) and performance was evaluated using NSE, NSE of log-transformed flows, R^2, and percent error in annual flow estimations. In Rattlesnake Canyon, this included 2005–2008, excluding water year 2007 due to missing streamflow data (i.e., simulation years 0, 1, and 3), and performance was evaluated using NSE, NSE of log-transformed flows, R^2, and percent error in annual flow estimations over the streamflow recession periods (similar to the approach used for calibration).

TABLE 3. Allometric ratios used for allocating C and N to various RHESSys state variables based on measured leaf area index (LAI).

Parameter	Pine	Shrub	Deciduous	Grass
Specific leaf area	3.30†	11.11‡	25‡	25.30‡
Root:leaf	1.40‡	1.40‡	1.20‡	1‡
Stem:leaf	0.98‡	0.22‡	2.20‡	
Root:stem	0.27§	0.29‡	0.22‡	
New live wood: new total wood	0.07‡	1.00‡	0.16‡	
C:N leaf	81.22§	35‡	25‡	25‡
C:N root	90.90§	58‡	48‡	50‡
C:N live wood	90.90§	58‡	48‡	
C:N deadwood	876‡	730‡	550‡	

†Averaged from Cregg (1994), Law et al. (2003), and Sala et al. (2005).
‡White et al. (2000).
§Ter-Mikaelian and Korzukhin (1997).

Finally, to explore how a chosen target variable can influence ecohydrologic projections, we ran five patch-scale simulations in Johnson Creek that were initialized with various targets. These simulations incorporated a single modeling unit that used mean elevation, slope, aspect, and soil parameter values for the watershed. To initialize these simulations for a young *P. ponderosa* stand, we obtained literature-based target values for either LAI, stem wood C, canopy height, stand age, or all four variables simultaneously (Law et al. 2001). While these initializations ignore spatial heterogeneity, they demonstrate the potential for using a range of targets in future applications where maps of such variables are available. Following initialization, we ran five 50-yr simulations and compared projections of cumulative ET and NPP during the first 10 yr (the period when fluxes varied most among targets).

RESULTS

In Johnson Creek, mean LAI calculated from an August 2001 Landsat scene was 2.94 (SE = 0.00 SE, SD = 0.81) for patches classified as pine, 1.77 (SE = 0.00, SD = 0.58) for those classified as grass, 1.55 (SE = 0.00, SD = 0.59) for shrub, and 2.85 (SE = 0.02, SD = 0.92) for deciduous. In Rattlesnake Canyon, where the AVIRIS footprint was much smaller (i.e., 12 m as compared to 30 m) and where vegetation cover was entirely shrub, mean LAI calculated in August 2004 was 2.12 (SE = 0.01, SD = 0.98).

Because we used LAI as the defining layer to initialize C and N pools, the approach using allometric relationships produced initial LAI estimates that essentially match those derived from remote sensing values in both Johnson Creek and Rattlesnake Canyon. The spin-up to steady state produced the lowest correspondence between initialized and remotely sensed values (Fig. 3a, b). The target-driven spin-up approach produced initial LAI estimates that corresponded well with remote sensing estimates; however, some patches never reached their targets (Fig. 3a, b). Although allometric relationships and the target-driven spin-up approach produced similar LAI distributions among patches in both watersheds, C allocation to leaves, stems,

and roots varied among all three methods. In both watersheds, spin-up to steady state produced much larger stem and root C pools relative to the two methods using remote sensing (Figs. 4a–c, 5a–c).

50-yr fluxes in Johnson Creek

Over the course of the 50-yr post-initialization runs in Johnson Creek, mean annual LAI values varied by up to 25% among the three methods, with allometric relationships producing the highest long-term estimates, and spin-up to steady state producing the lowest, due to the greater respiration costs associated with the large initial stem and root C pools (Fig. 6a). Also, LAI values declined rapidly in the first three years after initialization with allometric relationships, reflecting some instability with the allocation of initial C and N pools (Fig. 6a). Belowground C stores and root depth were 200–300% greater for the simulation that was initialized using spin-up to steady state (Fig. 6b). While root depth remained relatively stable in the simulation that followed spin-up to steady state, it increased slowly in simulations following the other two initialization approaches (Fig. 6b). Greater root biomass and depth following spin-up to steady state resulted in increased ET and decreased streamflow during the first 20 yr of the 50-yr simulation (Fig. 7a, b). ET was also slightly lower, and streamflow slightly higher for the simulation that was initialized using target-driven spin-up relative to the one that was initialized with allometric relationships. N export was highest for the simulation that was initialized using the target-driven method, followed by the one using spin-up to steady state (despite reduced streamflow in the steady-state method; Fig. 7c). This corresponded with decreased NPP (for simulations initialized using spin-up to steady state; Fig. 7d). In the first years of simulation (i.e., water years 2002–2006; Figs. 6b, 8b), the new target-driven spin-up approach produced the best correspondence between modeled and observed streamflow (Table 4).

Rattlesnake Canyon

In Rattlesnake Canyon, 50-yr LAI estimates were lower for the simulation initialized using spin-up to steady state (Fig. 8a). LAI values began to converge for the three methods over the course of the 50-yr simulations, as root C increased for the two methods that used remote sensing. Initial root depth in Rattlesnake Canyon was greatest for the simulation using spin-up to steady state, followed by the simulation initialized using allometric relationships, and lowest following target-driven spin-up (Fig. 8b). However, simulated root depth following target-driven initialization surpassed root depth following initialization with allometric relationships within the first two years of simulation. Despite the differences in C allocation among initialization methods, mean annual ET, streamflow, and N export projections were relatively similar over the 50-yr simulation period (Fig. 9a–c). NPP was slightly lower for the simulation initialized using spin-up to steady state (Fig. 9d). In water years 2005, 2006, and 2008 (Fig. 8b), model performance (i.e., correspondence between modeled and observed streamflow during recession periods) varied among metrics, with
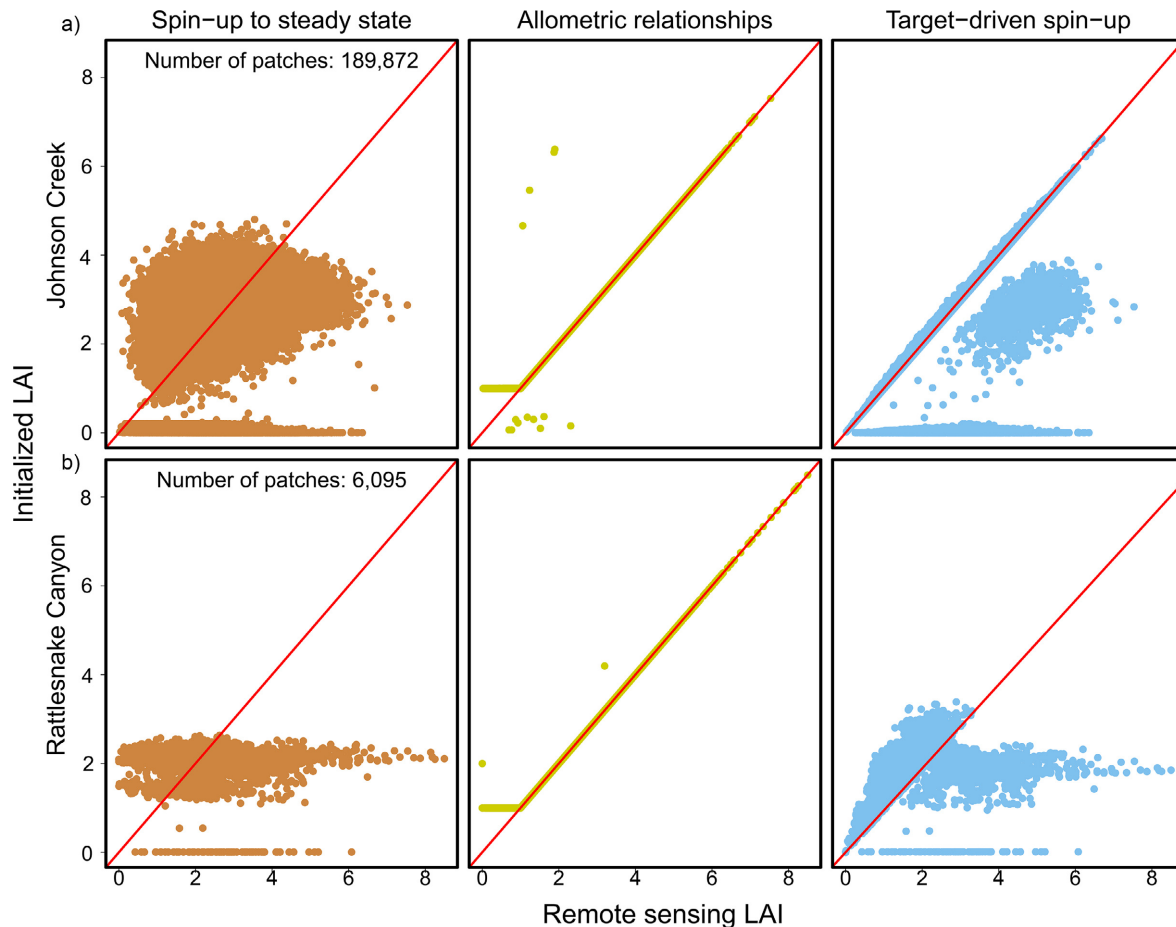
Fig. 3. Comparisons of target leaf area index (LAI) from remote sensing and initialized LAI in (a) Johnson Creek and (b) Rattlesnake Canyon using each of the three initialization methods: spin-up to steady state, remote sensing with allometric relationships, and target-driven spin-up. Points represent mean LAI for each patch.

the new target-driven method producing the best log of NSE, and allometric relationships producing the lowest percent error (Table 4).

Target comparisons

Spin-up time varied among simulations using different target variables to initialize a young *P. ponderosa* patch; LAI and canopy height targets were met most quickly, while age targets took the longest (Table 5). Projections of cumulative ET over the first 10 yr of simulation varied up to 19% when using different targets for initialization, while cumulative NPP varied up to 18% (Table 5). Cummulative NPP and ET were greater for simulations initialized using stem wood and age targets relative to LAI and canopy height.

DISCUSSION

Initialization provides critical constraints on model behavior; model estimates of C, N, and water fluxes vary depending on which approach is used. In Johnson Creek, spin-up to steady state produced large, stable, stem wood and root C pools, leading to higher ET, and streamflow projections that were 31% below field observations

(Table 4). Johnson Creek has a complex fire history, typical of watersheds in the Inland Northwest (Fig. 1a), resulting in heterogeneous above- and belowground C stores that are not captured by a steady-state approach. If streamflow is used to subsequently calibrate model drainage parameters, calibration may adjust for this error. However, this compensation would result in biased drainage parameters, producing the "right answers for the wrong reasons" (Kirchner 2006) and potentially biasing the use of the model for future scenarios. Overall, differences between steady state and remote sensing-based estimates of biogeochemical and hydrologic fluxes reflect key differences in the ecological function of heterogeneous landscapes that include younger aggrading stands as compared to homogeneously aged, mature forests.

In Rattlesnake Canyon, on the other hand, there were no major differences in mean annual ET, streamflow, or N export among the three methods (Fig. 9a–c). The similarity between the approaches using remote sensing and spin-up to steady state likely occurred because chaparral tends to experience large, stand-replacing fires, resulting in relatively homogeneous stand ages across watersheds. In August 2004, Rattlesnake Canyon had not burned for 40 yr, which is almost the length of time the watershed was spun up for the
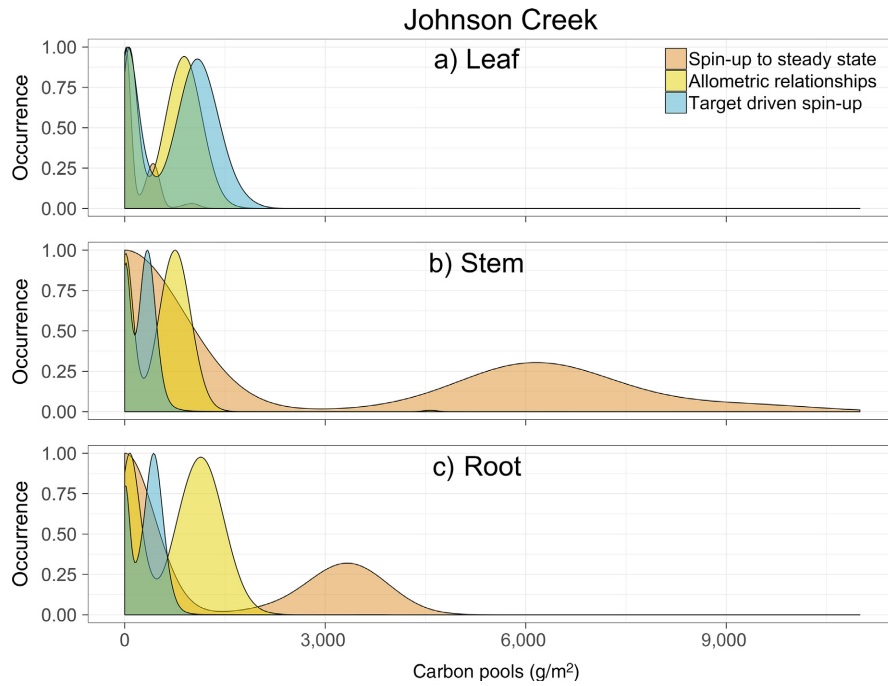
Johnson Creek

Fig. 4. Occurance of (a) leaf C, (b) stem C (including live and dead stems), and (c) root C (including fine roots as well as live and dead coarse roots) allocation values across patches in Johnson Creek immediately after initialization. For visualization purposes, the plots are rescaled such that the peak density equals 1.
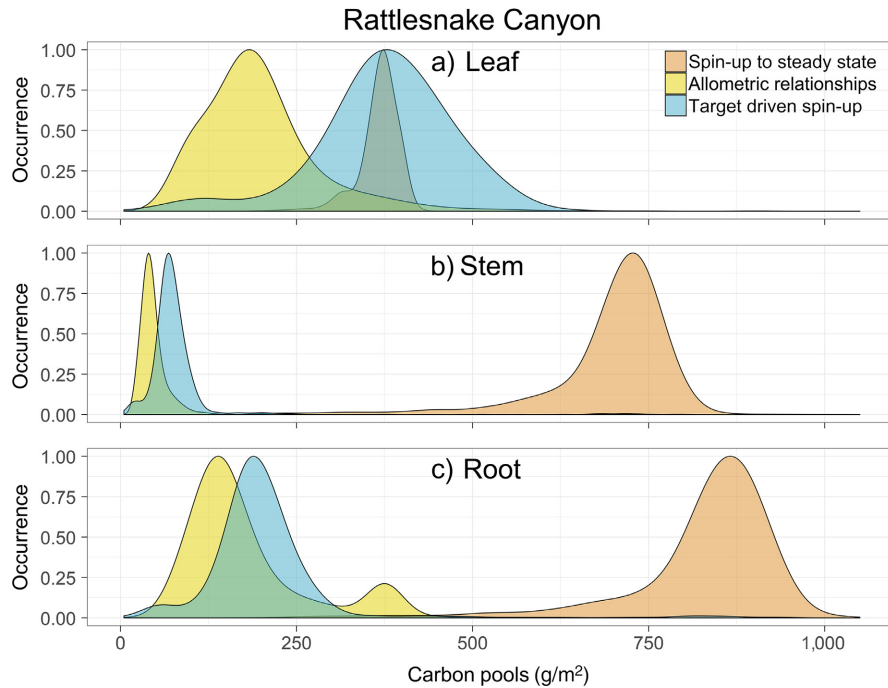
Rattlesnake Canyon

Fig. 5. Occurrence of (a) leaf C, (b) stem C (including live and dead stems), and (c) root C (including fine roots as well as live and dead coarse roots) allocation values across patches in Rattlesnake Canyon immediately after initialization. For visualization purposes, the plots are rescaled such that the peak density equals 1.

steady-state approach. Therefore, initializing Rattlesnake Canyon with 2004 as the remote sensing scene led to C and N distributions that were functionally similar to the spin-up to steady-state approach. Also, because post-disturbance hydrologic recovery in chaparral usually occurs within 1–4 yr (Verkaik et al. 2013), differences in vegetation structure among mature stands, such as those modeled here, are not likely to have significant ecohydrologic effects.
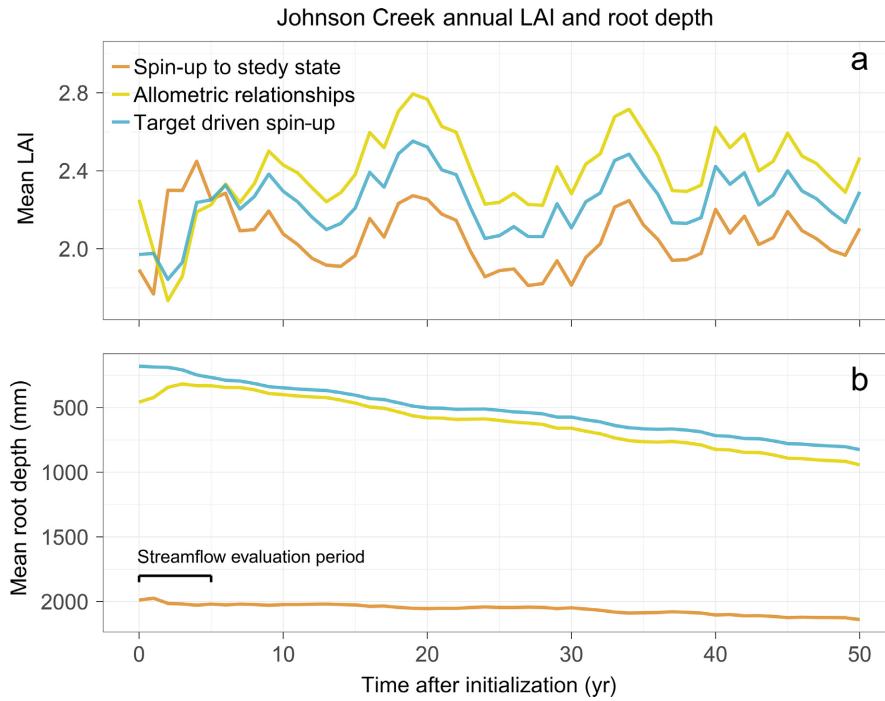
Johnson Creek annual LAI and root depth

FIG. 6. (a) Leaf area index (LAI) and (b) rooting depth in Johnson Creek over 50 yr of simulation using each of the three initialization approaches: spin-up to steady state, remote sensing with allometric relationships, and target-driven spin-up.
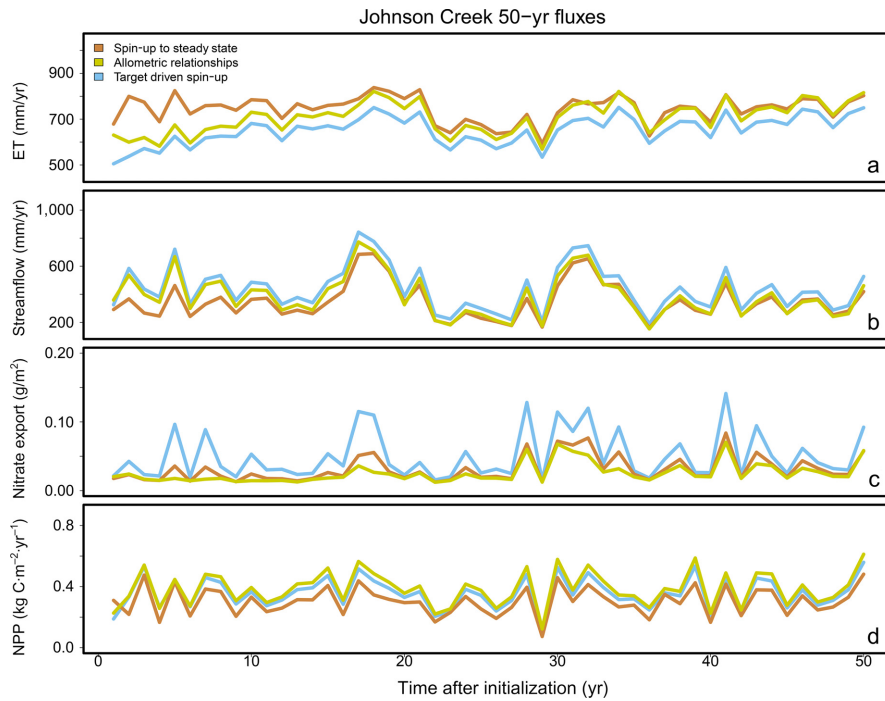
Johnson Creek 50−yr fluxes

FIG. 7. In Johnson Creek, 50-yr fluxes following each of the three initialization approaches: spin-up to steady state, remote sensing with allometric relationships, and target-driven spin-up for (a) total annual evapotranspiration (ET), (b) total annual streamflow, (c) N export, and (d) net primary productivity (NPP).

Although mean annual hydrologic fluxes were similar among methods in Rattlesnake Canyon, the simulation initialized using target-driven spin-up did a slightly better job capturing daily streamflow observations compared to the one using allometric relationships (Table 4). While the discrepancy was small in this study, it may be larger in other chaparral watersheds where allometric relationships are often poor predictors of shrub growth. In chaparral,
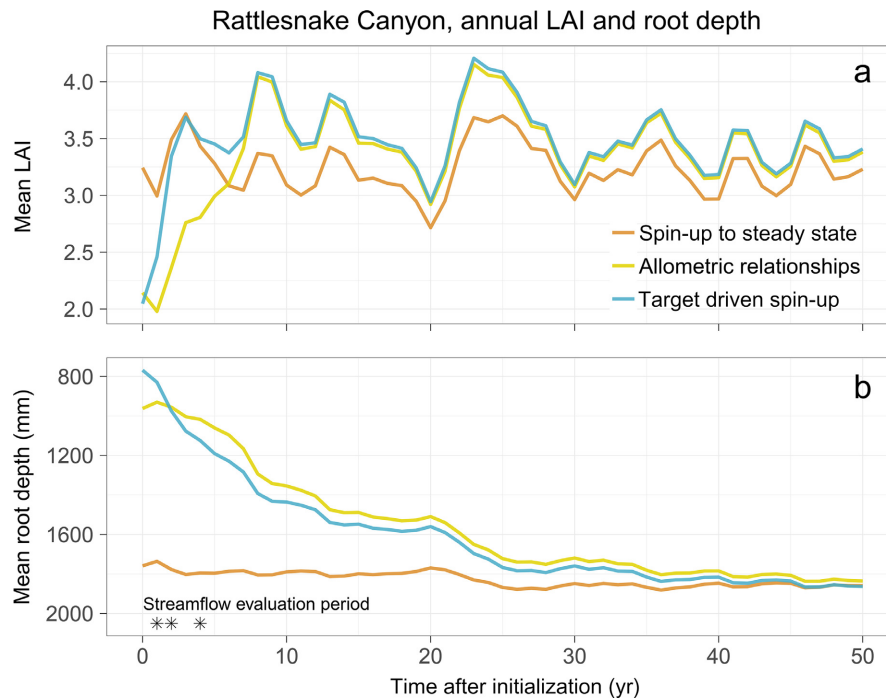
FIG. 8. (a) Leaf area index (LAI) and (b) rooting depth in Rattlesnake Canyon over 50 yr of simulation using each of the three initialization approaches: spin-up to steady state, remote sensing with allometric relationships, and target-driven spin-up. The * indicate years that were used to evaluate the correspondence between observed and modeled streamflow.

TABLE 4. Performance statistics for comparisons between modeled and observed streamflow during the simulation period spanning real climate data and prior to any wildfires; i.e., water years 2002–2006 in Johnson Creek (i.e., simulation years 0–5 in Fig. 6), and 2005–2008 (excluding water year 2007 due to missing streamflow records) in Rattlesnake Canyon (i.e., simulation years 0, 1, and 3 in Fig. 8).

Method	NSE	log(NSE)	R^2	Error (%)
Johnson Creek				
Spin-up to steady state	0.66	0.86	0.90	−32.43
Allometric relationships	0.78	0.85	0.90	−4.86
Target-driven spin-up	0.79	0.86	0.89	1.46
Rattlesnake Canyon				
Spin-up to steady state		0.40		11.33
Allometric relationships		0.42		4.48
Target-driven spin-up		0.44		9.84

Notes: Performance was evaluated for each method in Johnson Creek using the Nash-Sutcliffe efficiency metric (NSE), NSE of log-transformed flows (to evaluate low flow periods), R^2 for the Pearson correlation coefficient between daily observed and modeled flow, and percent error in annual flow estimations. In Rattlesnake Canyon, performance was evaluated using NSE of log-transformed flows and percent error in annual flow estimations during streamflow recession periods.

a single shrub can have several basal stems that can be meters apart, and region-specific allometric relationships often do not exist due to logistical constraints (Brown 1976, Uyeda et al. 2016). Overall however, it appears that all three approaches did an adequate job of projecting hydrologic fluxes in the more homogenously aged chaparral watershed, with performance similar to that achieved in previous studies (Shields and Tague 2012, Chen 2016).

Spin-up to steady state

When using the traditional spin-up to steady-state approach to initialize C and N pools, LAI projections were initially lower than in simulations using the other two methods, due to the greater respiration costs associated with the large stem and root C pools (Figs. 6a, 8a). Although estimates converged among the three approaches over the course of the 50-yr simulations, most rapidly in Rattlesnake Canyon (Figs. 6a, 8a), there were still large and more persistent differences in the way C was allocated to plant pools in both watersheds (Figs. 4a–c, 5a–c, 6b, 8b). In Johnson Creek, large differences C allocation led to divergent projections of biogeochemical and hydrologic fluxes. These differences result from complex linkages among C, N, and water cycling that change as forests grow (Law et al. 2001).

During first few decades of simulation after spin-up to steady state in Johnson Creek, ET was higher (Fig. 7a) and streamflow was lower (Fig. 7b) than in simulations using the other two initialization methods. This coincided with elevated N export in the steady-state approach relative to the approach using allometric relationships (Fig. 7c). In general, N-export is a function of both mineral N availability and how much water is available for transport (Gallo et al. 2015). At steady state, Nmexport is elevated even when streamflow is low, reflecting greater N availability. At equilibrium, N does not generally limit plant growth; therefore, N outputs are equal to inputs (Vitousek and Reiners 1975). For simulations initialized with allometric relationships, which included growing patches with high ET, N uptake was greater, and even though more water was available for transport (i.e., streamflow was higher), N export was lower.
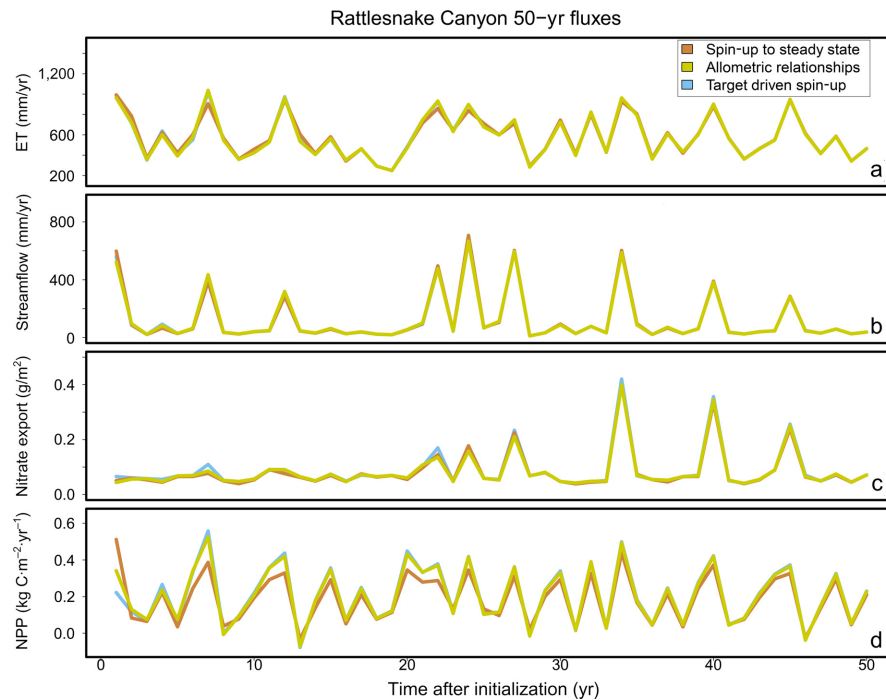
FIG. 9. In Rattlesnake Canyon, 50-yr fluxes following each of the three initialization approaches: spin-up to steady state, remote sensing with allometric relationships, and target-driven spin-up for (a) total annual evapotranspiration (ET), (b) total annual streamflow, (c) N export, and (d) net primary productivity (NPP).

TABLE 5. Results from comparison of patch-scale runs using different targets for initialization.

Target	Observed	Years to initialize	Cumulative ET (mm/10 yr)	Cumulative NPP (kg C·m^{-2}· 10 yr^{-1})
Leaf area index	1	10	7,022	4.23
Stem wood C (kg/m^2)	0.52	14	8,593	5.12
Height (m)	4	10	7,022	4.64
Age (yr)	15	15	8,638	5.17
All†	See above	15	8,638	5.17

Notes: Target values were obtained for young *Pinus ponderosa* stand in the Pacific Northwest, USA (Law et al. 2003). Following initialization, we ran a set of 10-yr simulations to compare cumulative evapotranspiration (ET) and net primary productivity (NPP).

†All four targets were used for this run. At the patch scale the "all" initialization will match whichever target takes the longest to spin up; in this case age. At the watershed scale, this could vary among patches.

Allometric relationships

Combining observations with allometric relationships can improve our ability to capture non-equilibrium conditions. However, when using literature-derived allometric relationships to initialize C and N pools in Johnson Creek, LAI values declined rapidly during the first few years after initialization (Fig. 6a). This type of instability can occur when root C is too small to access sufficient water to support the photosynthesis rates that are necessary to maintain initialized leaf and stem C stores (Running and Coughlan

1988). In such cases, photosynthesis will be consistently lower than respiration and turnover losses, leading to a rapid decline in vegetation biomass. Over time, the model corrects these instabilities by reducing plant biomass and regrowing more functionally stable stands. Thus, the simulation that was initialized using allometric relationships in Johnson Creek eventually (after 8 yr) recovered its initialized LAI (Fig. 6a). However, many patches crashed and gradually recovered in the first few years of simulation, suggesting that allometric relationships may not be useful for shorter-term studies, particularly those focused on the first decade of recovery from disturbance.

Surprisingly, in Rattlesnake Canyon where allometric relationships were expected to be less reliable, far fewer patches crashed in the first few years of simulation. This suggests that initialization approach can be particularly important in watersheds with heterogeneous stand ages like Johnson Creek. However, even in watersheds with more homogeneous vegetation, allometric relationships can still lead to C and N distributions that are unstable depending on local environmental conditions. We designed the new target-driven spin-up method to account for both resource heterogeneity and instability that can result from using empirical relationships.

Target-driven spin-up

Target-driven spin-up provides a more mechanistic initialization strategy that still accounts for landscape heterogeneity and non-steady-state conditions. Unlike the allometric relationship approach, when plant C stores develop over the course of spin-up, aboveground biomass is limited to what

can be supported by root C. We found that, in Johnson Creek, the target-driven approach led to streamflow projections that corresponded most closely with field observations (Table 4). However, our study also illustrates limitations to using LAI to define targets. For example, in Johnson Creek, the coarser spatial resolution of Landsat (i.e., 30 m) and potential scaling mismatches between vegetation classified using the National Land Cover Database and actual groundcover likely yielded mixed pixels, especially between the two dominant vegetation types: grass and pine. Some patches classified as grass may actually contain a mixture of grass and pine species, yielding higher radiometrically averaged NDVI in August relative to NDVI expected for grass only. Similarly, pine patches that also contain grass cover may have lower-than-expected NDVI if the grass proportion of a mixed pixel is large enough to dampen the signal (Eklundh et al. 2003). In RHESSys, grass patches with overestimated LAI would likely never reach their targets, and would therefore spin up for the maximum number of years (200 in the current study), while mixed pine patches would meet their targets too soon.

In addition to the potential scaling errors, there may also be error associated with using LAI as a target. Although LAI projections began to converge for the three methods over the course of the 50-yr simulations, root C and root depth remained different, particularly in Johnson Creek (Figs. 6a, b, 8a,b), which led to 17% less streamflow over the course of the 50-yr simulations. While two systems can have similar LAI, one may be at steady state while the other is actively growing belowground. Also, local differences in resource availability can lead to differences in the amount of C that plants allocate to roots (Running and Gower 1991). This raises two questions: (1) can using LAI as a target cause root biomass to be underestimated in some cases? And, therefore, (2) is LAI the best variable to use for target-driven spin-up?

LAI integrates several processes relating to C allocation and resource availability, and is a widely available data product. Thus, if models reasonably represent landscape patterns and soil processes, LAI should provide suitable targets for estimating plant C stores. Leaf Area Index is also mechanistically useful in models like RHESSys that account for processes that vary with canopy depth, such as light extinction and rainfall interception (Turner et al. 2004), and it is relatively easy to calculate from multispectral satellite data because it generally correlates well with vegetation indices such as the normalized difference vegetation index (NDVI). However, there are some caveats to consider when using LAI as a target. For one, LAI estimates do not always reflect fine-scale age differences in dense forests because the relationship between LAI and NDVI tends to be asymptotic, with LAI levels saturating at values between 3 and 5 (Turner et al. 1999). Also, vegetation tends to recover its pre-disturbance LAI more quickly than many other C stores. In our patch-scale comparisons, we found that targets for LAI and canopy height were met much more quickly than those for age and stem wood C (Table 5). This led to 10-yr cumulative ET estimates that were 18–19% lower for simulations initialized with LAI and canopy height. Simulations initialized using stem wood C and age targets on the other hand produced to similar estimates (within 1%).

Age is a preferred target variable because it eliminates multiple sources of error that are involved in modeling LAI and other target C stores (e.g., estimation of photosynthesis rates, parameterization of specific leaf area, carbon allocation strategies, and the timing of phenology). However, accurate estimates of stand age rely on documentation rather than post-hoc measurements. Thus stand age estimates are unlikely to be available for most locations and simulation start times; while products that can be derived from post-hoc observations and remote sensing such as LAI, height, or stem wood C are available for most sites. We found that stem wood C can provide spin-up targets that match most closely with stand age. Therefore, as spatial estimates of stem wood C become more widely available, they may provide more realistic targets than LAI. Despite its limitations however, LAI estimates can still be useful for generating coarse spin-up targets because they vary among older and more recently disturbed patches.

Here, we used Landsat and AVIRIS-derived LAI estimates to provide proof-of-concept for a target-driven approach. Using LAI allowed us to compare projections between the target-driven approach and an existing method using remote sensing (i.e., allometric relationships). Most patches in the two study watersheds were at or below the saturation threshold for NDVI. This occurred in Johnson Creek because most patches burned in one or more of several fires that occurred in recent decades, while in Rattlesnake Canyon, the mean LAI for our 2004 scene was around two. Also, in mature chaparral, shrub LAI is typically below 3.5 (Tague et al. 2009). However, an advantage of the new approach is that it can readily use finer resolution, and more-accurate target variables when available. Also, the target-driven approach allows multiple targets to be set simultaneously, which can further improve estimates of C allocation.

Other remote sensing products for generating targets

Hyperspectral remote sensing data (e.g., from AVIRIS) can be used to estimate other C and N stores used in landscape models, for example, RHESSys models leaf N, which is a major constituent of chlorophyll. The absorbance properties of leaf N are reflected in the spectral signature of leaves (Blackburn 2007). Because leaf N both influences and is influenced by heterogeneous environmental and physiological processes across a watershed, it may be an effective target variable for constraining C and N allocation during spin-up. However, there is still a great deal of uncertainty in how to interpret leaf biochemistry from spectral properties, as there can be significant error associated with radiative transfer through three-dimensional canopies (Knyazikhin et al. 2013). Where available, lidar estimates of canopy structure may help disentangle vertical effects on these relationships.

Lidar measures the three-dimensional vertical structure of vegetation with high accuracy (Dubayah and Drake 2000). Previous studies have developed methods for using lidar data to initialize C cycling models. For example, Hurtt et al. (2004) developed look up tables that linked canopy height with model projections of changes in forest structure using the Ecosystem Demography (ED) model.

Then, in combination with lidar data, they used these tables to initialize forest C stores. Expanding on this, Thomas et al. (2008) used detailed topographic and climate data to link canopy height with modeled above ground C stores for unique elevation bands across a mountainous watershed. This allowed them to initialize elevation-specific C stores with lidar, thus accounting for the effects of elevational gradients on C cycling processes. Both methods are useful for empirically constraining the state of initial aboveground C pools.

Our new target-driven approach extends and generalizes these previous methods by providing a framework for incorporating multiple data sources at high spatial resolution, while also ensuring that the initialized C stores are consistent with the mechanistic model. Thus, similar to the approaches above, target-driven spin-up can account for local environmental conditions using lidar or other remote sensing products to initialize C stores while also, in some cases, increasing model stability. Lidar data can be used to generate targets such as canopy height, stem wood C, and biomass. Like LAI, biomass is a meaningful target variable for C studies because biomass recovery after disturbance directly influences net ecosystem C exchange (Houghton et al. 2009). In addition, biomass measurements from lidar can be used to generate non-asymptotic estimates of LAI (Lefsky et al. 1999), providing another option for generating spin-up targets. However, a current limitation is that lidar data sets are expensive, and those designed to measure canopy structure are relatively rare. Further, unless lidar data are acquired and processed following specific methods, they do not discriminate between live and dead trees, which is critical for initializing models.

Incorporating soil pools

While C allocation to roots influences biogeochemical and ecohydrologic processes at landscape scales, other belowground properties also play a role in these dynamics. One of the largest sources of uncertainty in ecohydrologic modeling is how soil properties, including hydraulic conductivity, water storage, and C pool dynamics vary across watersheds (Kumar et al. 2010). To address the first two categories of uncertainty, many models (including RHESSys) calibrate soil drainage and storage parameters using daily streamflow statistics. For soil C and N pools however, models typically assume near steady-state conditions (Schimel et al. 1997, Morales et al. 2005) and initialize pools using methods similar to the spin-up to steady-state approach used for vegetation. These steady-state assumptions are unrealistic in many terrestrial ecosystems because it can take millennia for soil C and N stores to reach equilibrium following disturbance (Wardle et al. 1997, Cannell and Thornley 2003, Wutzler and Reichstein 2007).

While the new spin-up method can easily be extended to use soil pools as targets, spatially explicit soil C data are currently very limited, and not easily obtained with remote sensing. In addition to a lack of data, it can be difficult to translate field measurements of soil C to state variables in models. This is because, unlike vegetation state variables, modeled soil C and N pools are not easy to differentiate in the field (Smith et al. 2002). Most models use a set of kinetically defined C and N pools, with varying recalcitrance, to simplify the processes involved in exponential decay. In these models, decomposition removes a constant fraction from each pool at every time step as a function of its decomposition rate and environmental conditions (Wutzler and Reichstein 2007). In nature, on the other hand, organic matter is a complex mixture of materials, and there is no unequivocal way to distinguish between fast, intermediate, and slow-cycling pools; often decomposition rates are determined as much by microbial access to C compounds as they are by the molecular composition of those compounds (Stockmann et al. 2013). Nevertheless, this multi-pool abstraction allows models to adequately project C fluxes at decadal time scales, especially given the uncertainty associated with the distribution of belowground C stores (Parton 1996, Tague and Band 2001, Nemani et al. 2005).

Other approaches have been developed to account for soil stores that are not at steady state and may be useful in combination with a vegetation-focused, target-driven spin-up. For example, Wutzler and Reichstein (2007) and (Carvalhais et al. 2008) developed an initialization approach using a "relaxed steady-state assumption." This approach scales soil C pools, using a parameter derived from eddy covariance C flux data, following a normal spin-up to equilibrium, allowing users to more-realistically initialize non-steady-state conditions at landscape scales. (Hashimoto et al. 2011), then expanded the method to account for feedbacks with soil N pools, using a "slow-relaxation scheme." In this scheme, the scaling parameter introduced by (Carvalhais et al. 2008) and an "easing factor" are used to adjust C pools during spin-up, allowing for longer-term interactions between soil C and N. While both approaches improve model estimates of net-ecosystem productivity, the slow-relaxation scheme accounts for the effects of ecosystem N dynamics, such as mineralization rates, on productivity when ecosystems are not at steady state, while also overcoming model instability that can occur with the C-only approach (Hashimoto et al. 2011). These approaches may work in tandem with the new target-driven spin-up method when landscape-scale data are available. As spatial data become more widely available, and as computing capabilities improve, we can continue to refine the way we simulate and initialize complex belowground processes at watershed scales.

Future work

In addition to developing strategies for better-initializing soil stores, future studies should focus on evaluating which metrics provide the best initialization of post-disturbance plant dynamics. In the current study, the target-driven spin-up approach improved model performance in Johnson Creek. However, at the patch-scale, model projections varied when using different target variables to initialize plant C and N stores (e.g., LAI vs. stem wood C; Table 5), and suggested that using stem wood C rather than LAI may improve initialization, provided that accurate estimates are available. It is likely that the utility different initialization targets will vary across a range of sites, reflecting local ecological conditions. An important next step is to evaluate watershed-scale model performance following initialization with a range of target variables. With this knowledge, and as satellite

systems continue to improve, we can further increase our modeling accuracy.

Another current limitation of many C cycling models (including RHESSys) is that they do not account for species shifts that can occur following disturbance. This limitation can add error to projections of biogeochemical cycles, for example, during the early stages of succession (Hurtt et al. 2010). Several ecosystem biogeochemical models have addressed this limitation by incorporating submodels for temporal shifts in plant functional type (PFT; e.g., Moorcroft et al. 2001, Bond-Lamberty et al. 2005, Keane et al. 2011). It may also be possible to use remote sensing approaches to initialize spatial PFT transitions across landscapes (Hakkenberg et al. 2018). Incorporating PFT shifts into models that employ mechanistic, target-driven initialization may further improve biogeochemical projections in disturbance-prone watersheds.

Conclusions

In his famous paper on predictability, Lorenz (1972) found that the tiny rounding errors in climate models could produce vastly different long-term forecasts. Similarly, in watershed models, which incorporate many complex interactions and feedbacks, small changes in initial conditions can have large effects on decadal-scale projections. Advances in sensors, satellite systems, and our ability to process large data sets provide an opportunity to better initialize landscape heterogeneity and disturbance history in models (Raupach et al. 2005). To do this successfully, however, we must develop coherent methods for combining these large spatial data sets with process-based models. Our approach focused on developing a framework for synthesizing multiple remote sensing products with mechanistic spin-up methods to better initialize disturbance history in watersheds.

In Johnson Creek (the larger, more-heterogeneous watershed), remote sensing provided the most realistic initial conditions. And though initializing with allometric relationships provided starting LAI values that corresponded most precisely with remote sensing, it allocated corollary C and N pools using empirical rather than mechanistic relationships, resulting in less stable estimates of LAI and streamflow in the first decade of simulation. These instabilities can make allometric relationships unreliable for initializing studies that focus on the first decade of recovery from disturbance. The target-driven spin-up approach, on the other hand, used remote sensing to constrain mechanistic biogeochemical and hydrologic processes in the model. While there is some error associated with both remote sensing and modeling estimates of LAI, the target-driven approach appears to provide a useful crosswalk between them. The primary benefit of the new approach, however, is that it is designed to incorporate a greater diversity of data sets, going beyond the traditional use of LAI and allometric relationships. While our proof of concept combined Landsat and AVIRIS-derived LAI with the process-based model RHESSys, the framework can readily use other remote sensing products (Table 1), and can be applied to other spatially distributed models, allowing it to improve with advancing technology. Combining these state-of-the-art tools may help us to evaluate global change issues, including climate change, drought, and habitat degradation, in ways that were previously impossible.

Literature Cited

Abatzoglou, J. T. 2013. Development of gridded surface meteorological data for ecological applications and modelling. International Journal of Climatology 33:121–131.

Abatzoglou, J. T., and T. J. Brown. 2012. A comparison of statistical downscaling methods suited for wildfire applications. International Journal of Climatology 32:772–780.

Abdelnour, A., R. B. McKane, M. Stieglitz, F. Pan, and Y. Cheng. 2013. Effects of harvest on carbon and nitrogen dynamics in a Pacific Northwest forest catchment. Water Resources Research 49:1292–1313.

Ackerly, D. D. 2004. Adaptation, niche conservatism, and convergence: comparative studies of leaf evolution in the California chaparral. American Naturalist 163:654–671.

Ajami, H., M. F. McCabe, J. P. Evans, and S. Stisen. 2014. Assessing the impact of model spin-up on surface water-groundwater interactions using an integrated hydrologic model. Water Resources Research 50:2636–2656.

Antonarakis, A. S., S. S. Saatchi, R. L. Chazdon, and P. R. Moorcroft. 2010. Using Lidar and Radar measurements to constrain predictions of forest ecosystem structure and function. Ecological Applications 21:1120–1137.

Arkle, R. S., and D. S. Pilliod. 2010. Prescribed fires as ecological surrogates for wildfires: A stream and riparian perspective. Forest Ecology and Management 259:893–903.

Baret, F., A. Olioso, J. L. Luciani, and J. F. Hanocq. 1989. Estimation de l'énergie photosynthétiquement active absorbée par une culture de blé à partir de données radiométriques. Agronomie 9:885–895.

Beighley, R. E., T. Dunne, and J. M. Melack. 2005. Understanding and modeling basin hydrology: interpreting the hydrogeological signature. Hydrological Processes 19:1333–1353.

Berner, L. T., and B. E. Law. 2016. Plant traits, productivity, biomass and soil properties from forest sites in the Pacific Northwest, 1999–2014. Scientific Data 3:1–15.

Blackburn, G. A. 2007. Hyperspectral remote sensing of plant pigments. Journal of Experimental Botany 58:855–867.

Bond-Lamberty, B., S. T. Gower, D. E. Ahl, and P. E. Thornton. 2005. Reimplementation of the Biome-BGC model to simulate successional change. Tree Physiology 25:413–424.

Brown, J. K. 1976. Estimating shrub biomass from basal stem diameters. Canadian Journal of Forest Research 6:153–158.

Cannell, M. G. R., and J. H. M. Thornley. 2003. Ecosystem productivity is independent of some soil properties at equilibrium. Plant and Soil 257:193–204.

Carvalhais, N., et al. 2008. Implications of the carbon cycle steady state assumption for biogeochemical modeling performance and inverse parameter retrieval. Global Biogeochemical Cycles 22: GB2007.

Chen, X. 2016. Factors affecting the streamflow and in-stream nitrate concentration in semi-arid areas: sub-surface flow-generation, vertical distribution of soil nitrate and drainage properties, and the connectivity of impervious areas. Dissertation. University of California, Santa Barbara, Santa Barbara, California, USA.

Coughlan, J. C., and J. L. Dungan. 1997. Combining remote sensing and forest ecosystem modeling: an example using the Regional HydroEcological Simulation System (RHESSys). Pages 135–158 *in* H. Shimoda, H. L. Gholz, and K. Nakane, editors. The use of remote sensing in the modeling of forest productivity. Springer Netherlands, Dordrecht, The Netherlands.

Cregg, B. M. 1994. Carbon allocation, gas exchange, and needle morphology of Pinus ponderosa genotypes known to differ in growth and survival under imposed drought. Tree Physiology 14:883–898.

Daly, C., R. P. Neilson, and D. L. Phillips. 1994. A statistical-topographic model for mapping climatological precipitation over mountainous terrain. Journal of Applied Meteorology 33:140–158.

Dickinson, R. E., M. Shaikh, R. Bryant, and L. Graumlich. 1998. Interactive canopies for a climate model. Journal of Climate 11:2823–2836.

Dubayah, R. O., and J. B. Drake. 2000. Lidar remote sensing for forestry. Journal of Forestry 98:44–46.

Eidenshink, J., B. Schwind, K. Brewer, Z. L. Zhu, B. Quayle, and S. Howard. 2007. A project for monitoring trends in burn severity. Fire Ecology 3:4.

Eklundh, L., K. Hall, H. Eriksson, J. Ardö, and P. Pilesjö. 2003. Investigating the use of Landsat thematic mapper data for estimation of forest leaf area index in southern Sweden. Canadian Journal of Remote Sensing 29:349–362.

Farquhar, G. D., and S. Von Caemmerer. 1982. Modelling of photosynthetic response to environmental conditions. Pages 549–587 *in* O. L. Lange, P. S. Nobel, C. B. Osmond, H. Ziegler, editors. Physiological plant ecology II. Springer, Berlin, Germany.

Gallo, E. L., T. Meixner, H. Aoubid, K. A. Lohse, and P. D. Brooks. 2015. Combined impact of catchment size, land cover, and precipitation on streamflow and total dissolved nitrogen: a global comparative analysis. Global Biogeochemical Cycles 29:2015GB005154.

Gamon, J. A., C. B. Field, M. L. Goulden, K. L. Griffin, A. E. Hartley, G. Joel, J. Peñuelas, and R. Valentini. 1995. Relationships between NDVI, canopy structure, and photosynthesis in three Californian vegetation types. Ecological Applications 5:28–41.

Garcia, E. S., C. L. Tague, and J. S. Choate. 2013. Influence of spatial temperature estimation method in ecohydrologic modeling in the Western Oregon Cascades. Water Resources Research 49:1611–1624.

Garcia, E. S., C. L. Tague, and J. S. Choate. 2016. Uncertainty in carbon allocation strategy and ecophysiological parameterization influences on carbon and streamflow estimates for two western US forested watersheds. Ecological Modelling 342:19–33.

Garson, D. C., and B. Lacaze. 2003. Monitoring Leaf Area Index of Mediterranean oak woodlands: comparison of remotely-sensed estimates with simulations from an ecological process-based model. International Journal of Remote Sensing 24:3441–3456.

Goetz, S. J., A. Baccini, N. T. Laporte, T. Johns, W. Walker, J. Kellndorfer, R. A. Houghton, and M. Sun. 2009. Mapping and monitoring carbon stocks with satellite observations: a comparison of methods. Carbon Balance and Management 4:2.

Gonzalez, P., G. P. Asner, J. J. Battles, M. A. Lefsky, K. M. Waring, and M. Palace. 2010. Forest carbon densities and uncertainties from Lidar, QuickBird, and field measurements in California. Remote Sensing of Environment 114:1561–1575.

Goodale, C. L., J. D. Aber, and W. H. McDowell. 2000. The long-term effects of disturbance on organic and inorganic nitrogen export in the White Mountains, New Hampshire. Ecosystems 3:433–450.

Green, R. O., et al. 1998. Imaging spectroscopy and the airborne visible/infrared imaging spectrometer (AVIRIS). Remote Sensing of Environment 65:227–248.

Hakkenberg, C. R., R. K. Peet, D. L. Urban, and C. Song. 2018. Modeling plant composition as community continua in a forest landscape with LiDAR and hyperspectral remote sensing. Ecological Applications 28:177–190.

Hanan, E. J., C. M. D'Antonio, D. A. Roberts, and J. P. Schimel. 2016a. Factors regulating nitrogen retention during the early stages of recovery from fire in coastal chaparral ecosystems. Ecosystems 19:910–926.

Hanan, E. J., J. P. Schimel, K. Dowdy, and C. M. D'Antonio. 2016b. Effects of substrate supply, pH, and char on net nitrogen mineralization and nitrification along a wildfire-structured age gradient in chaparral. Soil Biology and Biochemistry 95:87–99.

Hanan, E. J., C. (Naomi) Tague, and J. P. Schimel. 2017. Nitrogen cycling and export in California chaparral: the role of climate in shaping ecosystem responses to fire. Ecological Monographs 87:76–90.

Hashimoto, S., M. Wattenbach, and P. Smith. 2011. A new scheme for initializing process-based ecosystem models by scaling soil carbon pools. Ecological Modelling 222:3598–3602.

Homer, C., J. Dewitz, L. Yang, S. Jin, P. Danielson, G. Xian, J. Coulston, N. Herold, J. Wickham, and K. Megown. 2015. Completion of the 2011 National Land Cover Database for the conterminous United States-Representing a decade of land cover change information. Photogrammetric Engineering and Remote Sensing 81:345–354.

Houghton, R. A., F. Hall, and S. J. Goetz. 2009. Importance of biomass in the global carbon cycle. Journal of Geophysical Research: Biogeosciences 114:G00E03.

Hurtt, G. C., R. Dubayah, J. Drake, P. R. Moorcroft, S. W. Pacala, J. B. Blair, and M. G. Fearon. 2004. Beyond potential vegetation: combining lidar data and a height-structured model for carbon studies. Ecological Applications 14:873–883.

Hurtt, G. C., J. Fisk, R. Q. Thomas, R. Dubayah, P. R. Moorcroft, and H. H. Shugart. 2010. Linking models and data on vegetation structure. Journal of Geophysical Research: Biogeosciences 115:G00E10.

Hyndman, D. W. 1983. The Idaho batholith and associated plutons, Idaho and Western Montana. Geological Society of America Memoirs 159:213–240.

Jarvis, P. G. 1976. The interpretation of the variations in leaf water potential and stomatal conductance found in canopies in the field. Philosophical Transactions of the Royal Society B 273:593–610.

Jones, H. G. 2013. Plants and microclimate: a quantitative approach to environmental plant physiology. Cambridge University Press, Cambridge, UK.

Kashian, D. M., W. H. Romme, D. B. Tinker, M. G. Turner, and M. G. Ryan. 2006. Carbon storage on landscapes with stand-replacing fires. BioScience 56:598–606.

Keane, R. E., R. A. Loehman, and L. M. Holsinger. 2011. The FireBGCv2 landscape fire succession model: a research simulation platform for exploring fire and vegetation dynamics. General Technical Report. United States Department of Agriculture Forest Service, Rocky Mountain Research Station, Washington, D.C., USA.

Kirchner, J. W. 2006. Getting the right answers for the right reasons: linking measurements, analyses, and models to advance the science of hydrology. Water Resources Research 42:W03S04.

Knicker, H. 2007. How does fire affect the nature and stability of soil organic nitrogen and carbon? A review. Biogeochemistry 85:91–118.

Knyazikhin, Y., et al. 2013. Hyperspectral remote sensing of foliar nitrogen content. Proceedings of the National Academy of Sciences USA 110:E185–E192.

Kumar, S., M. Sekhar, D. V. Reddy, and M. S. Mohan Kumar. 2010. Estimation of soil hydraulic properties and their uncertainty: comparison between laboratory and field experiment. Hydrological Processes 24:3426–3435.

Law, B. E., P. E. Thornton, J. Irvine, P. M. Anthoni, and S. Van Tuyl. 2001. Carbon storage and fluxes in ponderosa pine forests at different developmental stages. Global Change Biology 7:755–777.

Law, B. E., O. J. Sun, J. Campbell, S. Van Tuyl, and P. E. Thornton. 2003. Changes in carbon storage and fluxes in a chronosequence of ponderosa pine. Global Change Biology 9:510–524.

Lefsky, M. A., W. B. Cohen, S. A. Acker, G. G. Parker, T. A. Spies, and D. Harding. 1999. Lidar remote sensing of the canopy structure and biophysical properties of Douglas-fir western hemlock forests. Remote Sensing of Environment 70:339–361.

Loehman, R. A., E. Reinhardt, and K. L. Riley. 2014. Wildland fire emissions, carbon, and climate: Seeing the forest and the trees – A cross-scale assessment of wildfire and carbon dynamics in fire-prone, forested ecosystems. Forest Ecology and Management 317:9–19.

Lorenz, E. 1972. Predictability: does the flap of a butterflys wing in Brazil set off a tornado in Texas? Presented before the American Association for the Advancement of Science.

McGuire, A. D., J. M. Melillo, L. A. Joyce, D. W. Kicklighter, A. L. Grace, B. Moore, and C. J. Vorosmarty. 1992. Interactions between carbon and nitrogen dynamics in estimating net primary productivity for potential vegetation in North America. Global Biogeochemical Cycles 6:101–124.

McMichael, C. E., A. S. Hope, D. A. Roberts, and M. R. Anaya. 2004. Post-fire recovery of leaf area index in California chaparral: a remote sensing-chronosequence approach. International Journal of Remote Sensing 25:4743–4760.

Megahan, W. F., J. P. Potyondy, and K. A. Seyedbagheri. 1992. Best management practices and cumulative effects from sedimentation in the South Fork Salmon River: an Idaho Case Study. Pages 401–414 in R. J. Naiman, editor. Watershed management. Springer, New York, New York, USA.

Mitchell, K. E., et al. 2004. The multi-institution North American Land Data Assimilation System (NLDAS): utilizing multiple GCIP products and partners in a continental distributed hydrological modeling system. Journal of Geophysical Research: Atmospheres 109:D07S90.

Monteith, J. L. 1965. Evaporation and environment. Symposia of the Society for Experimental Biology 19:4.

Moorcroft, P. R., G. C. Hurtt, and S. W. Pacala. 2001. A method for scaling vegetation dynamics: the ecosystem demography model (ED). Ecological Monographs 71:557–586.

Morales, P., et al. 2005. Comparing and evaluating process-based ecosystem model predictions of carbon and water fluxes in major European forest biomes. Global Change Biology 11: 2211–2233.

Moritz, M. A. 2003. Spatiotemporal analysis of controls on shrubland fire regimes: age dependency and fire hazard. Ecology 84:351–361.

Motallebi, A., and A. Kangur. 2016. Are allometric relationships between tree height and diameter dependent on environmental conditions and management? Trees 30:1429–1443.

Nash, J. E., and J. V. Sutcliffe. 1970. River flow forecasting through conceptual models part I—A discussion of principles. Journal of Hydrology 10:282–290.

Thornton, Peter E., Steven W. Running, and E. R. Hunt. "Biome-BGC: terrestrial ecosystem process model, Version 4.1. 1." ORNL DAAC (2005).

NRCS. 2015. Description of Gridded Soil Survey Geographic (gSSURGO) Database | NRCS. https://www.nrcs.usda.gov/wps/portal/nrcs/detail/soils/survey/?cid=nrcs142p2_053627

Parton, W. J. 1996. The CENTURY model. Pages 283–291 in D. S. Powlson, P. Smith, and J. U. Smith, editors. Evaluation of soil organic matter models. Springer, Berlin, Heidelberg.

Pastor, J., and W. M. Post. 1986. Influence of climate, soil moisture, and succession on forest carbon and nitrogen cycles. Biogeochemistry 2:3–27.

Pietsch, S. A., and H. Hasenauer. 2006. Evaluating the self-initialization procedure for large-scale ecosystem models. Global Change Biology 12:1658–1669.

Raupach, M. R., P. J. Rayner, D. J. Barrett, R. S. DeFries, M. Heimann, D. S. Ojima, S. Quegan, and C. C. Schmullius. 2005. Model–data synthesis in terrestrial carbon observation: methods, data requirements and data uncertainty specifications. Global Change Biology 11:378–397.

Rollins, M. G. 2009. LANDFIRE: a nationally consistent vegetation, wildland fire, and fuel assessment. International Journal of Wildland Fire 18:235–249.

Running, S. W., and J. C. Coughlan. 1988. A general model of forest ecosystem processes for regional applications I. Hydrologic balance, canopy gas exchange and primary production processes. Ecological Modelling 42:125–154.

Running, S. W., and S. T. Gower. 1991. FOREST-BGC, A general model of forest ecosystem processes for regional applications. II. Dynamic carbon allocation and nitrogen budgets. Tree Physiology 9:147–160.

Running, S. W., R. R. Nemani, and R. D. Hungerford. 1987. Extrapolation of synoptic meteorological data in mountainous terrain and its use for simulating forest evapotranspiration and photosynthesis. Canadian Journal of Forest Research 17:472–483.

Sala, A., G. D. Peters, L. R. McIntyre, and M. G. Harrington. 2005. Physiological responses of ponderosa pine in western Montana to thinning, prescribed fire and burning season. Tree Physiology 25:339–348.

Schimel, D. S., B. H. Braswell, and W. J. Parton. 1997. Equilibration of the terrestrial water, nitrogen, and carbon cycles. Proceedings of the National Academy of Sciences USA 94:8280–8283.

Shi, M., Z.-L. Yang, D. M. Lawrence, R. E. Dickinson, and Z. M. Subin. 2013. Spin-up processes in the Community Land Model version 4 with explicit carbon and nitrogen components. Ecological Modelling 263:308–325.

Shields, C. A., and C. L. Tague. 2012. Assessing the role of parameter and input uncertainty in ecohydrologic modeling: implications for a semi-arid and urbanizing coastal California catchment. Ecosystems 15:775–791.

Shugart, H. H. 1984. A theory of forest dynamics: the ecological implications of forest succession models. Springer-Verlag, Berlin, Germany.

Smith, F. W., D. A. Sampson, and J. N. Long. 1991. Notes: Comparison of leaf area index estimates from tree allometrics and measured light interception. Forest Science 37:1682–1688.

Smith, J. U., P. Smith, R. Monaghan, and A. J. MacDonald. 2002. When is a measured soil organic matter fraction equivalent to a model pool? European Journal of Soil Science 53:405–416.

Stockmann, U., et al. 2013. The knowns, known unknowns and unknowns of sequestration of soil organic carbon. Agriculture, Ecosystems & Environment 164:80–99.

Tague, C. L., and L. E. Band. 2001. Evaluating explicit and implicit routing for watershed hydro-ecological models of forest hydrology at the small catchment scale. Hydrological Processes 15:1415–1439.

Tague, C. L., and L. E. Band. 2004. RHESSys: Regional Hydro-ecologic simulation system—an object-oriented approach to spatially distributed modeling of carbon, water, and nutrient cycling. Earth Interactions 8:1–42.

Tague, C., C. McMichael, A. Hope, J. Choate, and R. Clark. 2004. Application of the RHESSys model to a California semiarid shrubland watershed. JAWRA Journal of the American Water Resources Association 40:575–589.

Tague, C., L. Seaby, and A. Hope. 2009. Modeling the eco-hydrologic response of a Mediterranean type ecosystem to the combined impacts of projected climate change and altered fire frequencies. Climatic Change 93:137–155.

Ter-Mikaelian, M. T., and M. D. Korzukhin. 1997. Biomass equations for sixty-five North American tree species. Forest Ecology and Management 97:1–24.

Thomas, R. Q., G. C. Hurtt, R. Dubayah, and M. H. Schilz. 2008. Using lidar data and a height-structured ecosystem model to estimate forest carbon stocks and fluxes over mountainous terrain. Canadian Journal of Remote Sensing 34:S351–S363.

Thornton, P. E., and N. A. Rosenbloom. 2005. Ecosystem model spin-up: Estimating steady state conditions in a coupled terrestrial carbon and nitrogen cycle model. Ecological Modelling 189:25–48.

Turner, D. P., W. B. Cohen, R. E. Kennedy, K. S. Fassnacht, and J. M. Briggs. 1999. Relationships between leaf area index and Landsat TM spectral vegetation indices across three temperate zone sites. Remote Sensing of Environment 70:52–68.

Turner, D. P., S. V. Ollinger, and J. S. Kimball. 2004. Integrating remote sensing and ecosystem process models for landscape- to regional-scale analysis of the carbon cycle. BioScience 54:573–584.

Uyeda, K. A., D. A. Stow, J. F. O'Leary, C. Tague, and P. J. Riggan. 2016. Chaparral growth-ring analysis as an indicator of stand biomass development. International Journal of Wildland Fire 25:1086–1092.

Verkaik, I., M. Rieradevall, S. D. Cooper, J. M. Melack, T. L. Dudley, and N. Prat. 2013. Fire as a disturbance in Mediterranean climate streams. Hydrobiologia 719:353–382.

Vitousek, P. M., and W. A. Reiners. 1975. Ecosystem succession and nutrient retention: a hypothesis. BioScience 25:376–381.

Vourlitis, G. L., G. Zorba, S. C. Pasquini, and R. Mustard. 2007. Carbon and nitrogen storage in soil and litter of southern Californian semi-arid shrublands. Journal of Arid Environments 70:164–173.

Wardle, D. A., O. Zackrisson, G. Hörnberg, and C. Gallet. 1997. The influence of island area on ecosystem properties. Science 277:1296–1299.

White, M. A., P. E. Thornton, S. W. Running, and R. R. Nemani. 2000. Parameterization and sensitivity analysis of the BIOME–BGC terrestrial ecosystem model: net primary production controls. Earth Interactions 4:1–85.

Wutzler, T., and M. Reichstein. 2007. Soils apart from equilibrium? Consequences for soil carbon balance modelling. Biogeosciences 4:125–136.

Xia, J. Y., Y. Q. Luo, Y.-P. Wang, E. S. Weng, and O. Hararuk. 2012. A semi-analytical solution to accelerate spin-up of a coupled carbon and nitrogen land model to steady state. Geoscientific Model Development 5:1259–1271.

DATA AVAILABILITY